



# CHORUS

This is the accepted manuscript made available via CHORUS. The article has been published as:

## Search for charmonium and charmoniumlike states in $Y(2S)$ radiative decays

X. L. Wang *et al.* (Belle Collaboration)

Phys. Rev. D **84**, 071107 — Published 28 October 2011

DOI: [10.1103/PhysRevD.84.071107](https://doi.org/10.1103/PhysRevD.84.071107)

# Search for charmonium and charmonium-like states in $\Upsilon(2S)$ radiative decays

X. L. Wang,<sup>13</sup> C. P. Shen,<sup>30</sup> C. Z. Yuan,<sup>13</sup> P. Wang,<sup>13</sup> I. Adachi,<sup>9</sup> H. Aihara,<sup>51</sup> D. M. Asner,<sup>40</sup> T. Aushev,<sup>17</sup> A. M. Bakich,<sup>45</sup> E. Barberio,<sup>29</sup> K. Belous,<sup>15</sup> B. Bhuyan,<sup>11</sup> A. Bozek,<sup>35</sup> M. Bračko,<sup>27,18</sup> T. E. Browder,<sup>8</sup> M.-C. Chang,<sup>4</sup> A. Chen,<sup>32</sup> B. G. Cheon,<sup>7</sup> K. Chilikin,<sup>17</sup> I.-S. Cho,<sup>55</sup> K. Cho,<sup>21</sup> Y. Choi,<sup>44</sup> J. Dalseno,<sup>28,47</sup> M. Danilov,<sup>17</sup> Z. Doležal,<sup>2</sup> S. Eidelman,<sup>1</sup> J. E. Fast,<sup>40</sup> M. Feindt,<sup>20</sup> V. Gaur,<sup>46</sup> Y. M. Goh,<sup>7</sup> J. Haba,<sup>9</sup> K. Hayasaka,<sup>30</sup> H. Hayashii,<sup>31</sup> Y. Hoshi,<sup>49</sup> Y. B. Hsiung,<sup>34</sup> H. J. Hyun,<sup>23</sup> T. Iijima,<sup>30</sup> A. Ishikawa,<sup>50</sup> R. Itoh,<sup>9</sup> M. Iwabuchi,<sup>55</sup> Y. Iwasaki,<sup>9</sup> T. Iwashita,<sup>31</sup> T. Julius,<sup>29</sup> J. H. Kang,<sup>55</sup> N. Katayama,<sup>9</sup> T. Kawasaki,<sup>37</sup> H. Kichimi,<sup>9</sup> H. J. Kim,<sup>23</sup> H. O. Kim,<sup>23</sup> J. B. Kim,<sup>22</sup> J. H. Kim,<sup>21</sup> K. T. Kim,<sup>22</sup> M. J. Kim,<sup>23</sup> Y. J. Kim,<sup>21</sup> K. Kinoshita,<sup>3</sup> B. R. Ko,<sup>22</sup> N. Kobayashi,<sup>41,52</sup> S. Koblitz,<sup>28</sup> P. Križan,<sup>25,18</sup> A. Kuzmin,<sup>1</sup> Y.-J. Kwon,<sup>55</sup> J. S. Lange,<sup>5</sup> S.-H. Lee,<sup>22</sup> J. Li,<sup>43</sup> X. R. Li,<sup>43</sup> Y. Li,<sup>54</sup> J. Libby,<sup>12</sup> C.-L. Lim,<sup>55</sup> C. Liu,<sup>42</sup> D. Liventsev,<sup>17</sup> R. Louvot,<sup>24</sup> D. Matvienko,<sup>1</sup> S. McOnie,<sup>45</sup> K. Miyabayashi,<sup>31</sup> H. Miyata,<sup>37</sup> Y. Miyazaki,<sup>30</sup> G. B. Mohanty,<sup>46</sup> R. Mussa,<sup>16</sup> Y. Nagasaka,<sup>10</sup> M. Nakao,<sup>9</sup> H. Nakazawa,<sup>32</sup> Z. Natkaniec,<sup>35</sup> S. Neubauer,<sup>20</sup> S. Nishida,<sup>9</sup> K. Nishimura,<sup>8</sup> O. Nitoh,<sup>53</sup> S. Ogawa,<sup>48</sup> T. Ohshima,<sup>30</sup> S. Okuno,<sup>19</sup> S. L. Olsen,<sup>43,8</sup> Y. Onuki,<sup>50</sup> P. Pakhlov,<sup>17</sup> G. Pakhlova,<sup>17</sup> H. Park,<sup>23</sup> H. K. Park,<sup>23</sup> T. K. Pedlar,<sup>26</sup> R. Pestotnik,<sup>18</sup> M. Petrič,<sup>18</sup> L. E. Piilonen,<sup>54</sup> M. Ritter,<sup>28</sup> S. Ryu,<sup>43</sup> H. Sahoo,<sup>8</sup> Y. Sakai,<sup>9</sup> T. Sanuki,<sup>50</sup> O. Schneider,<sup>24</sup> C. Schwanda,<sup>14</sup> K. Senyo,<sup>30</sup> O. Seon,<sup>30</sup> M. E. Sevier,<sup>29</sup> M. Shapkin,<sup>15</sup> T.-A. Shibata,<sup>41,52</sup> J.-G. Shiu,<sup>34</sup> B. Shwartz,<sup>1</sup> F. Simon,<sup>28,47</sup> P. Smerkol,<sup>18</sup> Y.-S. Sohn,<sup>55</sup> E. Solovieva,<sup>17</sup> S. Stanič,<sup>38</sup> M. Starič,<sup>18</sup> M. Sumihama,<sup>41,6</sup> G. Tatishvili,<sup>40</sup> Y. Teramoto,<sup>39</sup> K. Trabelsi,<sup>9</sup> M. Uchida,<sup>41,52</sup> S. Uehara,<sup>9</sup> Y. Unno,<sup>7</sup> S. Uno,<sup>9</sup> Y. Usov,<sup>1</sup> G. Varner,<sup>8</sup> C. H. Wang,<sup>33</sup> M.-Z. Wang,<sup>34</sup> Y. Watanabe,<sup>19</sup> E. Won,<sup>22</sup> B. D. Yabsley,<sup>45</sup> Y. Yamashita,<sup>36</sup> M. Yamauchi,<sup>9</sup> Z. P. Zhang,<sup>42</sup> and V. Zhilich<sup>1</sup>

(The Belle Collaboration)

<sup>1</sup>*Budker Institute of Nuclear Physics SB RAS and Novosibirsk State University, Novosibirsk 630090*

<sup>2</sup>*Faculty of Mathematics and Physics, Charles University, Prague*

<sup>3</sup>*University of Cincinnati, Cincinnati, Ohio 45221*

<sup>4</sup>*Department of Physics, Fu Jen Catholic University, Taipei*

<sup>5</sup>*Justus-Liebig-Universität Gießen, Gießen*

<sup>6</sup>*Gifu University, Gifu*

<sup>7</sup>*Hanyang University, Seoul*

<sup>8</sup>*University of Hawaii, Honolulu, Hawaii 96822*

<sup>9</sup>*High Energy Accelerator Research Organization (KEK), Tsukuba*

<sup>10</sup>*Hiroshima Institute of Technology, Hiroshima*

<sup>11</sup>*Indian Institute of Technology Guwahati, Guwahati*

<sup>12</sup>*Indian Institute of Technology Madras, Madras*

<sup>13</sup>*Institute of High Energy Physics, Chinese Academy of Sciences, Beijing*

<sup>14</sup>*Institute of High Energy Physics, Vienna*

<sup>15</sup>*Institute of High Energy Physics, Protvino*

<sup>16</sup>*INFN - Sezione di Torino, Torino*

<sup>17</sup>*Institute for Theoretical and Experimental Physics, Moscow*

<sup>18</sup>*J. Stefan Institute, Ljubljana*

<sup>19</sup>*Kanagawa University, Yokohama*

<sup>20</sup>*Institut für Experimentelle Kernphysik, Karlsruher Institut für Technologie, Karlsruhe*

<sup>21</sup>*Korea Institute of Science and Technology Information, Daejeon*

<sup>22</sup>*Korea University, Seoul*

<sup>23</sup>*Kyungpook National University, Taegu*

<sup>24</sup>*École Polytechnique Fédérale de Lausanne (EPFL), Lausanne*

<sup>25</sup>*Faculty of Mathematics and Physics, University of Ljubljana, Ljubljana*

<sup>26</sup>*Luther College, Decorah, Iowa 52101*

<sup>27</sup>*University of Maribor, Maribor*

<sup>28</sup>*Max-Planck-Institut für Physik, München*

<sup>29</sup>*University of Melbourne, School of Physics, Victoria 3010*

<sup>30</sup>*Nagoya University, Nagoya*

<sup>31</sup>*Nara Women's University, Nara*

<sup>32</sup>*National Central University, Chung-li*

<sup>33</sup>*National United University, Miao Li*

<sup>34</sup>*Department of Physics, National Taiwan University, Taipei*

<sup>35</sup>*H. Niewodniczanski Institute of Nuclear Physics, Krakow*

<sup>36</sup>*Nippon Dental University, Niigata*

<sup>37</sup>*Niigata University, Niigata*

<sup>38</sup>*University of Nova Gorica, Nova Gorica*

- <sup>39</sup>Osaka City University, Osaka  
<sup>40</sup>Pacific Northwest National Laboratory, Richland, Washington 99352  
<sup>41</sup>Research Center for Nuclear Physics, Osaka  
<sup>42</sup>University of Science and Technology of China, Hefei  
<sup>43</sup>Seoul National University, Seoul  
<sup>44</sup>Sungkyunkwan University, Suwon  
<sup>45</sup>School of Physics, University of Sydney, NSW 2006  
<sup>46</sup>Tata Institute of Fundamental Research, Mumbai  
<sup>47</sup>Excellence Cluster Universe, Technische Universität München, Garching  
<sup>48</sup>Toho University, Funabashi  
<sup>49</sup>Tohoku Gakuin University, Tagajo  
<sup>50</sup>Tohoku University, Sendai  
<sup>51</sup>Department of Physics, University of Tokyo, Tokyo  
<sup>52</sup>Tokyo Institute of Technology, Tokyo  
<sup>53</sup>Tokyo University of Agriculture and Technology, Tokyo  
<sup>54</sup>CNP, Virginia Polytechnic Institute and State University, Blacksburg, Virginia 24061  
<sup>55</sup>Yonsei University, Seoul

Using a sample of 158 million  $\Upsilon(2S)$  events collected with the Belle detector, charmonium and charmonium-like states with even charge parity are searched for in  $\Upsilon(2S)$  radiative decays. No significant  $\chi_{cJ}$  or  $\eta_c$  signal is observed and the following upper limits at 90% confidence level (C.L.) are obtained:  $\mathcal{B}(\Upsilon(2S) \rightarrow \gamma\chi_{c0}) < 1.0 \times 10^{-4}$ ,  $\mathcal{B}(\Upsilon(2S) \rightarrow \gamma\chi_{c1}) < 3.6 \times 10^{-6}$ ,  $\mathcal{B}(\Upsilon(2S) \rightarrow \gamma\chi_{c2}) < 1.5 \times 10^{-5}$ , and  $\mathcal{B}(\Upsilon(2S) \rightarrow \gamma\eta_c) < 2.7 \times 10^{-5}$ . No significant signal of any charmonium-like state is observed, and we obtain the limits  $\mathcal{B}(\Upsilon(2S) \rightarrow \gamma X(3872)) \times \mathcal{B}(X(3872) \rightarrow \pi^+\pi^-J/\psi) < 0.8 \times 10^{-6}$ ,  $\mathcal{B}(\Upsilon(2S) \rightarrow \gamma X(3872)) \times \mathcal{B}(X(3872) \rightarrow \pi^+\pi^-\pi^0J/\psi) < 2.4 \times 10^{-6}$ ,  $\mathcal{B}(\Upsilon(2S) \rightarrow \gamma X(3915)) \times \mathcal{B}(X(3915) \rightarrow \omega J/\psi) < 2.8 \times 10^{-6}$ ,  $\mathcal{B}(\Upsilon(2S) \rightarrow \gamma Y(4140)) \times \mathcal{B}(Y(4140) \rightarrow \phi J/\psi) < 1.2 \times 10^{-6}$ , and  $\mathcal{B}(\Upsilon(2S) \rightarrow \gamma X(4350)) \times \mathcal{B}(X(4350) \rightarrow \phi J/\psi) < 1.3 \times 10^{-6}$  at 90% C.L.

PACS numbers: 14.40.Pq, 14.40.Rt, 13.20.Gd

The data samples of the  $B$  factories have provided a wealth of experimental information on charmonium spectroscopy [1]. Below open charm threshold agreement between experimental mass measurements and predictions based upon potential models was recently demonstrated with high accuracy for the  $h_c$  [2, 3]. However, in the region above the open charm threshold, in addition to many conventional charmonium states, a number of charmonium-like states (the so-called “XYZ particles”) have been discovered with unusual properties. These may include exotic states, such as quark-gluon hybrids, meson molecules, and multi-quark states [1]. Many of these new states are established in a single production mechanism or in a single decay mode only. To better understand them, it is necessary to search for such states in more production processes and/or decay modes. States with  $J^{PC} = 1^{--}$  can be studied via initial state radiation (ISR) with the large  $\Upsilon(4S)$  data samples at BaBar or Belle, or via  $e^+e^-$  collisions directly at the peak energy at, for example, BESIII. For charge-parity-even charmonium states, radiative decays of the narrow  $\Upsilon$  states below the open bottom threshold can be examined.

The production rates of the  $P$ -wave spin-triplet  $\chi_{cJ}$  ( $J=0, 1, 2$ ) and  $S$ -wave spin-singlet  $\eta_c$  states in  $\Upsilon(1S)$  radiative decays have been calculated by Gao *et al.*; the rates in  $\Upsilon(2S)$  decays are estimated to be at the same level [4]. However, there are no such calculations or estimations for “XYZ particles” due to the limited knowledge of their nature.

In this paper, with the world largest data sample

taken at the  $\Upsilon(2S)$  peak, we report a search for the  $\chi_{cJ}$ ,  $\eta_c$ ,  $X(3872)$  [5],  $X(3915)$  [6], and  $Y(4140)$  [7] in  $\Upsilon(2S)$  radiative decays, extending our previous work on the  $\Upsilon(1S)$  sample [8] by using similar event selection criteria. In addition, the new structure  $X(4350)$  [9], which was observed as a 3.2 standard deviation ( $\sigma$ ) signal in  $\gamma\gamma \rightarrow \phi J/\psi$  is also searched for. As any charmonium state above  $\psi(2S)$  is expected to have a larger branching fraction for the E1/M1 transition to  $\psi(2S)$  than to  $J/\psi$  [10], we also search for states decaying into  $\gamma\psi(2S)$ .

The data used in this analysis include a 24.7 fb<sup>-1</sup> data sample collected at the  $\Upsilon(2S)$  peak and a 1.7 fb<sup>-1</sup> data sample collected at  $\sqrt{s} = 9.993$  GeV (off-resonance data) with the Belle detector [11] operating at the KEKB asymmetric-energy  $e^+e^-$  collider [12]. The number of the  $\Upsilon(2S)$  events is determined by counting the hadronic events in the data taken at the  $\Upsilon(2S)$  peak after subtracting the scaled continuum background from the off-resonance data. The selection criteria for hadronic events are validated with the off-resonance data by comparing the measured  $R$  value ( $R = \frac{\sigma(e^+e^- \rightarrow \text{hadrons})}{\sigma(e^+e^- \rightarrow \mu^+\mu^-)}$ ) with CLEO’s result [13]. The number of  $\Upsilon(2S)$  events is determined to be  $(158 \pm 4) \times 10^6$ , with the error dominated by the MC simulation of the  $\Upsilon(2S)$  decay dynamics using PYTHIA [14].

Well measured charged tracks and photon candidates are first selected. For a charged track, the impact parameters perpendicular to and along the beam direction with respect to the interaction point (IP) are required to be less than 0.5 cm and 4 cm, respectively, and the

transverse momentum should exceed 0.1 GeV/c in the laboratory frame. Information from different detector subsystems is combined to form a likelihood  $\mathcal{L}_i$  for each particle species [15]. A track with  $\mathcal{R}_K = \frac{\mathcal{L}_K}{\mathcal{L}_K + \mathcal{L}_\pi} > 0.6$  is identified as a kaon, while a track with  $\mathcal{R}_K < 0.4$  is treated as a pion. With this selection, the kaon (pion) identification efficiency is about 90% (96%), while 5% (6%) of kaons (pions) are misidentified as pions (kaons). The likelihood ratios  $\mathcal{R}_e$  and  $\mathcal{R}_\mu$  are defined similarly for electron [16] and muon [17] identification, respectively. A good neutral cluster is reconstructed as a photon if its electromagnetic calorimeter (ECL) shower does not match the extrapolation of any charged track and its energy is greater than 40 MeV. In the  $e^+e^-$  center-of-mass (C.M.) frame, the photon candidate with the maximum energy is taken to be the  $\Upsilon(2S)$  radiative decay photon (denoted as  $\gamma_R$ ), and its energy is required to be greater than 3.5 GeV. A 3.5 GeV photon energy corresponds to a particle of mass 5.5 GeV/c<sup>2</sup> produced in  $\Upsilon(2S)$  radiative decays.

We reconstruct  $J/\psi$  signals from  $e^+e^-$  or  $\mu^+\mu^-$  candidates. In order to reduce the effect of bremsstrahlung or final-state radiation, photons detected in the ECL within 0.05 radians of the original  $e^+$  or  $e^-$  direction are included in the calculation of the  $e^+/e^-$  momentum. For the lepton pair used to reconstruct  $J/\psi$ , at least one track should have  $\mathcal{R}_e > 0.95$  while the other should satisfy  $\mathcal{R}_e > 0.05$  in the  $e^+e^-$  mode; or one track should have  $\mathcal{R}_\mu > 0.95$  (in the  $\chi_{cJ}$  analysis, the other track should have  $\mathcal{R}_\mu > 0$ ) in the  $\mu^+\mu^-$  mode. The lepton pair identification efficiency is about 97% for  $J/\psi \rightarrow e^+e^-$  and 87% for  $J/\psi \rightarrow \mu^+\mu^-$ . In order to improve the  $J/\psi$  momentum resolution, a mass-constrained fit is then performed for  $J/\psi$  signals in the  $\gamma J/\psi$ ,  $\pi^+\pi^- J/\psi$ ,  $\pi^+\pi^-\pi^0 J/\psi$ , and  $\phi J/\psi$  modes. Different modes have similar  $J/\psi$  mass resolutions. The  $J/\psi$  signal region is defined as  $|M_{\ell^+\ell^-} - m_{J/\psi}| < 30 \text{ MeV}/c^2$  ( $\approx 2.5\sigma$ ), where  $m_{J/\psi}$  is the nominal mass of  $J/\psi$ . The  $J/\psi$  mass sidebands are defined as  $2.959 \text{ GeV}/c^2 < M_{\ell^+\ell^-} < 3.019 \text{ GeV}/c^2$  and  $3.175 \text{ GeV}/c^2 < M_{\ell^+\ell^-} < 3.235 \text{ GeV}/c^2$ , and are twice as wide as the signal region. For the  $\gamma\psi(2S)$  channel, the  $\psi(2S)$  is reconstructed from the  $\pi^+\pi^- J/\psi$  final state, with a mass constrained to the nominal  $\psi(2S)$  mass to improve its momentum resolution. To estimate the difference in the  $\psi(2S)$  mass resolution between MC simulation and data, the process  $e^+e^- \rightarrow \gamma_{\text{ISR}}\psi(2S)$  is selected as a reference sample, and the mass resolution is  $3.0 \pm 0.1 \text{ MeV}/c^2$  from data, and  $2.6 \text{ MeV}/c^2$  from MC simulation. The difference in the mass resolution is included when extracting the signal yields in the analyses below.

We search for the  $\chi_{cJ}$  in the  $\gamma J/\psi$  mode. The energy deposited by the  $\chi_{cJ}$  photon (denoted as  $\gamma_I$ , since its energy is much lower than that of  $\gamma_R$ ) is required to be greater than 150 MeV to reduce the large background from mis-reconstructed photons, and the total number of photons is required to be exactly two to suppress multi-photon backgrounds. The angle between the  $\gamma_R$  and  $\gamma_I$

should be larger than 18° to remove the background from split-off fake photons. To remove the ISR background  $e^+e^- \rightarrow \gamma_{\text{ISR}}\psi(2S) \rightarrow \gamma_{\text{ISR}}\gamma\chi_{cJ}$ , where a photon is missing, we require the square of the “mass recoiling against the  $\gamma_I$  and  $J/\psi$ ” ( $M_{\text{rec}}^2 = (P_{e^+e^-} - P_f)^2$ , here  $P_{e^+e^-}$  is the 4-momentum of the  $e^+e^-$  collision system, and  $P_f$  is the sum of the 4-momenta of the observed final state particles) to be within  $-0.5 \text{ GeV}^2/c^4$  and  $0.5 \text{ GeV}^2/c^4$ . This  $M_{\text{rec}}^2$  requirement is effective since this background has at least two missing photons and  $M_{\text{rec}}^2(\gamma_I J/\psi)$  tends to be large. Bhabha and dimuon background events with final-state radiative photons are further suppressed by removing events in which a photon is detected within a 18° cone around each charged track direction.

The  $\mu^+\mu^-$  mode shows a clear  $J/\psi$  signal, while the  $e^+e^-$  mode has some residual radiative Bhabha background. Figure 1 shows the  $\gamma_I J/\psi$  invariant mass distribution together with the background estimated from the  $J/\psi$  mass sidebands (normalized to the width of the  $J/\psi$  signal range) for the combined  $e^+e^-$  and  $\mu^+\mu^-$  modes after the above selection criteria are applied. Some ISR backgrounds with a correctly reconstructed  $J/\psi$  remain in the data. No  $\chi_{cJ}$  signal is observed.

A simultaneous fit to the signal region is performed with Breit-Wigner (BW) functions convolved with Gaussian resolution functions for the resonances and a second-order polynomial background term. The width of the Gaussian resolution function is fixed at  $7.9 \text{ MeV}/c^2$ , which is obtained by increasing the MC-simulated value by 10% to account for the difference between data and MC simulation. The masses and widths of the  $\chi_{cJ}$  resonances are fixed to their PDG values [19]. In the simultaneous fit, the ratio of the yields in the two  $J/\psi$  decay channels is fixed to  $\mathcal{B}_i \varepsilon_i$ , where  $\mathcal{B}_i$  is the  $J/\psi$  decay branching fraction for the  $e^+e^-$  mode or  $\mu^+\mu^-$  mode reported by the PDG [19], and  $\varepsilon_i$  is the MC-determined efficiency for this mode. The upper limit on the number ( $n^{\text{up}}$ ) of signal events at the 90% C.L. is calculated by solving the equation  $\frac{\int_0^{n^{\text{up}}} \mathcal{L}(x) dx}{\int_0^{+\infty} \mathcal{L}(x) dx} = 0.9$ , where  $x$  is the number of signal events, and  $\mathcal{L}(x)$  is the likelihood function depending on  $x$  from the fit to the data. The values of  $n^{\text{up}}$  are found to be 2.8, 3.1 and 7.6 for the  $\chi_{c0}$ ,  $\chi_{c1}$  and  $\chi_{c2}$ , respectively, when requiring the signal yields to be non-negative in the fit. We do not observe any structure at high masses, where excited  $\chi_{cJ}$  states are expected.

To search for a possible excited charmonium state in the  $\gamma_I \psi(2S)$  final state, a  $J/\psi$  candidate and two oppositely charged pion candidates are reconstructed. The  $\psi(2S)$  signal region is defined as  $3.67 \text{ GeV}/c^2 < M_{\pi^+\pi^- J/\psi} < 3.70 \text{ GeV}/c^2$ , and the  $\psi(2S)$  mass sidebands are defined as  $3.63 \text{ GeV}/c^2 < M_{\pi^+\pi^- J/\psi} < 3.66 \text{ GeV}/c^2$  and  $3.71 \text{ GeV}/c^2 < M_{\pi^+\pi^- J/\psi} < 3.74 \text{ GeV}/c^2$ . To suppress backgrounds with misconstructed photons, we require the energy of the  $\gamma_I$  to be higher than 75 MeV. To suppress the ISR background  $e^+e^- \rightarrow \gamma_{\text{ISR}}\psi(2S) \rightarrow \gamma_{\text{ISR}}\pi^+\pi^- J/\psi$ , we re-

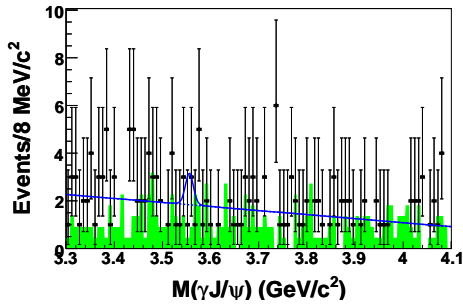


FIG. 1: (color online). The  $\gamma J/\psi$  invariant mass distribution. There is no  $\chi_{c0}$ ,  $\chi_{c1}$ , or  $\chi_{c2}$  signal observed. The solid curve is the best fit, the dashed curve is the background, and the shaded histogram is from the normalized  $J/\psi$  mass sidebands. The signal yield is required to be non-negative in the fit.

quire the  $M_{\text{rec}}^2(\gamma_l\psi(2S))$  to be within  $-0.5 \text{ GeV}^2/c^4$  and  $1.5 \text{ GeV}^2/c^4$  since  $M_{\text{rec}}^2$  for the ISR background tends to be shifted towards negative values.

The  $\gamma_l\psi(2S)$  invariant mass distribution after the above selection is shown in Fig. 2. There is no significant signal. However, a few events accumulate around  $3.82 \text{ GeV}/c^2$ , where the  $\gamma\psi(2S)$  decays of the  $\chi_{c0}(2P)$  and  $\eta_{c2}(1D)$  [10] are expected. A fit between  $3.75 \text{ GeV}/c^2$  and  $3.90 \text{ GeV}/c^2$  with a Gaussian to parameterize the signal shape yields a mass of  $(3.824 \pm 0.002) \text{ GeV}/c^2$  and a signal yield of  $5.5 \pm 2.7$  events corresponding to a statistical significance of  $1.8\sigma$ . The signal significance is determined by comparing the value of  $-2 \ln(L_0/L_{\text{max}})$  from the fit, with values from fits to 10,000 pseudo-experiments. Here  $L_0$  and  $L_{\text{max}}$  are the likelihoods of the fits without and with the signal, respectively. The upper limit on the product branching fraction  $\mathcal{B}(\Upsilon(2S) \rightarrow \gamma X) \times \mathcal{B}(X \rightarrow \gamma\psi(2S)) < 1.3 \times 10^{-5}$  at the 90% C.L. is determined following the procedure described below.

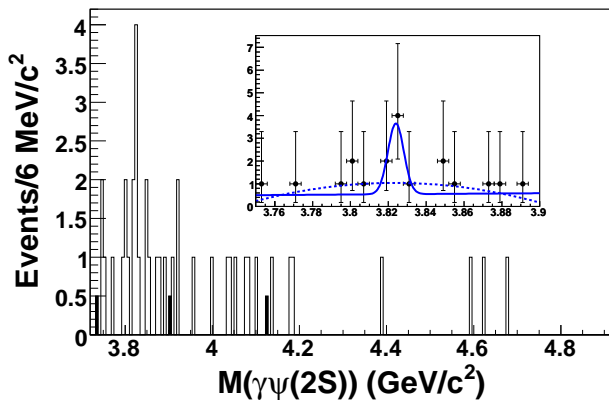


FIG. 2: (color online). The  $\gamma_l\psi(2S)$  invariant mass distribution. The open histogram is from the  $\psi(2S)$  signal mass region, the shaded histogram is from the normalized  $\psi(2S)$  mass sidebands. In the inset, the solid curve is the best fit between  $3.75 \text{ GeV}/c^2$  and  $3.90 \text{ GeV}/c^2$ , and the dashed curve is a fit with only a second-order polynomial to describe the background.

To search for the  $\eta_c$  signal in  $\Upsilon(2S)$  radiative decays, we reconstruct  $\eta_c$  candidates from the  $K_S^0 K^+ \pi^- + c.c.$ ,  $\pi^+ \pi^- K^+ K^-$ ,  $2(K^+ K^-)$ ,  $2(\pi^+ \pi^-)$ , and  $3(\pi^+ \pi^-)$  modes. Well measured charged tracks should be identified as pions or kaons, and the number of charged tracks is six for the  $3(\pi^+ \pi^-)$  final state and four for the other final states. In the  $K_S^0 K^+ \pi^- + c.c.$  mode,  $K_S^0$  candidates are reconstructed from  $\pi^+ \pi^-$  pairs with an invariant mass  $M_{\pi^+ \pi^-}$  within  $30 \text{ MeV}/c^2$  of the  $K_S^0$  nominal mass. A  $K_S^0$  candidate should have a displaced vertex and flight direction consistent with a  $K_S^0$  originating from the IP [18]. Events with leptons misidentified as pions in the  $\pi^+ \pi^- K^+ K^-$  and  $2(\pi^+ \pi^-)$  modes are removed by requiring  $\mathcal{R}_e < 0.9$  and  $\mathcal{R}_\mu < 0.9$  for the pion candidates. The value of  $M_{\text{rec}}^2$  for the hadronic daughters of the  $\eta_c$  candidate is required to be within  $-1 \text{ GeV}^2/c^4$  and  $1 \text{ GeV}^2/c^4$ .

After the selection described above, Fig. 3 shows the combined mass distribution of the hadronic final states for the five  $\eta_c$  decay modes. The large  $J/\psi$  signal is due to the ISR process  $e^+ e^- \rightarrow \gamma_{\text{ISR}} J/\psi$ , while the accumulation of events within the  $\eta_c$  mass region is small. The shaded histogram in Fig. 3 is the same distribution for the off-resonance data and is not normalized.

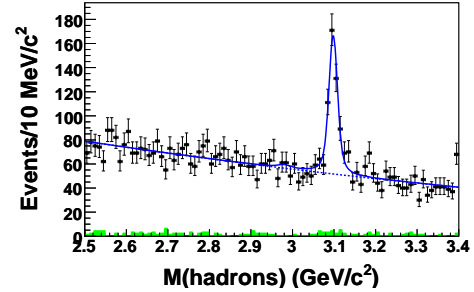


FIG. 3: (color online). The mass distribution for a sum of the five  $\eta_c$  decay modes. The solid curve is a sum of the corresponding functions obtained from a simultaneous fit to all the  $\eta_c$  decay modes, and the dashed curve is a sum of the background functions from the fit. The shaded histogram is a sum of the off-resonance events (not normalized). The  $J/\psi$  signal is produced via ISR rather than from a radiative decay of an  $\Upsilon(nS)$  resonance.

A simultaneous fit is performed to the five final states. The ratios of the  $\eta_c$  ( $J/\psi$ ) yields in all the channels are fixed to  $\mathcal{B}_i \varepsilon_i$ , where each  $\mathcal{B}_i$  is the  $\eta_c$  ( $J/\psi$ ) decay branching fraction for the  $i$ -th mode reported by the PDG [19], and  $\varepsilon_i$  is the MC-determined efficiency for this mode. The fit function contains a BW function convolved with a Gaussian resolution function (its resolution is fixed to  $7.9 \text{ MeV}/c^2$  from MC simulation) describing the  $\eta_c$  signal shape, another Gaussian function describing the  $J/\psi$  signal shape, and a second-order polynomial describing the background shape. The mass and width of the BW function are fixed to the PDG values [19] for the  $\eta_c$ . The results of the fit are shown in Fig. 3, where the solid curve is the sum of all the fit functions, and the dashed curve is the sum of the background functions. The fit yields  $14 \pm 20$   $\eta_c$  signal events corresponding to an upper

limit  $n^{\text{up}}$  of 44 at the 90% C.L. In addition, we obtain  $370 \pm 15$   $J/\psi$  signal events from the fit (in agreement with  $338 \pm 16$  expected from  $\gamma_{\text{ISR}} J/\psi$  production according to MC simulation), giving a mass of  $3098.1 \pm 0.7$   $\text{MeV}/c^2$ , which is consistent with the PDG value [19].

The selection criteria for  $\Upsilon(2S) \rightarrow \gamma_{\text{R}} X(3872)$ ,  $X(3872) \rightarrow \pi^+\pi^- J/\psi$  are similar to those used for ISR  $\pi^+\pi^- J/\psi$  events in  $\Upsilon(4S)$  data [20]. We require that one  $J/\psi$  candidate be reconstructed, two well-identified  $\pi$ 's have an invariant mass greater than  $0.35$   $\text{GeV}/c^2$ , and that  $M_{\text{rec}}^2(\pi^+\pi^- J/\psi)$  be within the range between  $-1$   $\text{GeV}^2/c^4$  and  $1$   $\text{GeV}^2/c^4$ . To suppress the ISR  $\pi^+\pi^- J/\psi$  background, we require that the polar angle of the  $\gamma_{\text{R}}$  candidate satisfy  $|\cos\theta| < 0.9$  in the  $e^+e^-$  C.M. frame. Except for a few residual ISR produced  $\psi(2S)$  signal events, only a small number of events appear in the  $\pi^+\pi^- J/\psi$  invariant mass distribution, as shown in Fig. 4(a). There is no accumulation of events in the  $X(3872)$  mass region. Fitting using a signal shape from the MC sample and a first-order polynomial function as the background shape, the upper limit  $n^{\text{up}}$  for the number of signal events is determined to be 3.6 at the 90% C.L.

We also search for the  $X(3872)$  and  $X(3915)$  in the  $\pi^+\pi^-\pi^0 J/\psi$  mode. We select  $\pi^+$ ,  $\pi^-$ , and  $J/\psi$  candidates in the  $X(3872) \rightarrow \pi^+\pi^- J/\psi$  mode (with the requirement on the  $\pi^+\pi^-$  invariant mass greater than  $0.35$   $\text{GeV}/c^2$  removed) and a  $\pi^0$  candidate from a pair of photons with invariant mass within  $10$   $\text{MeV}/c^2$  of the  $\pi^0$  nominal mass. Here the  $\pi^0$  mass resolution is about  $4$   $\text{MeV}/c^2$  from MC simulation. Figure 4(b) shows the  $\pi^+\pi^-\pi^0 J/\psi$  invariant mass distribution, where the open histogram is the MC expectation for the  $X(3872)$  signal, plotted with an arbitrary normalization. Using the same fit method as in  $X(3872) \rightarrow \pi^+\pi^- J/\psi$ , we determine  $n^{\text{up}}$  for the number of  $X(3872)$  signal events to be 4.2 at the 90% C.L. Figure 4(c) shows the scatter plot of  $m(\pi^+\pi^-\pi^0 J/\psi)$  versus  $m(\pi^+\pi^-\pi^0)$  from data, where the region indicated by the ellipse corresponds to the  $\pm 3\sigma$  mass regions of  $m(\pi^+\pi^-\pi^0 J/\psi)$  and  $m(\pi^+\pi^-\pi^0)$  from the  $X(3915) \rightarrow \omega J/\psi$  decay. There is one event with  $m(\pi^+\pi^-\pi^0 J/\psi)$  at  $3.923$   $\text{GeV}/c^2$  and  $m(\pi^+\pi^-\pi^0)$  at  $0.790$   $\text{GeV}/c^2$  from  $\Upsilon(2S)$  data, as shown in the ellipse. Assuming that the number of background events is zero, the upper limit  $n^{\text{up}}$  for the number of  $X(3915)$  signal events is 4.4 at the 90% C.L.

We search for the  $Y(4140)$  and the  $X(4350)$  in the  $\phi J/\psi$  mode. The selection criteria are very similar to those in the analysis of  $X(3872) \rightarrow \pi^+\pi^- J/\psi$  described above and the  $\phi$  is reconstructed from a  $K^+K^-$  pair. According to MC simulation, the  $\phi$  signal region is defined as  $1.01$   $\text{GeV}/c^2 < M_{K^+K^-} < 1.03$   $\text{GeV}/c^2$ . The number of well measured charged tracks is required to be exactly four. After applying all of the above event selection criteria, there is no clear  $J/\psi$  or  $\phi$  signal. Nor are there candidate events in the  $Y(4140)$  or  $X(4350)$  mass regions. The upper limits on the number of  $Y(4140)$  and  $X(4350)$  signal events are both 2.3 at the 90% C.L.

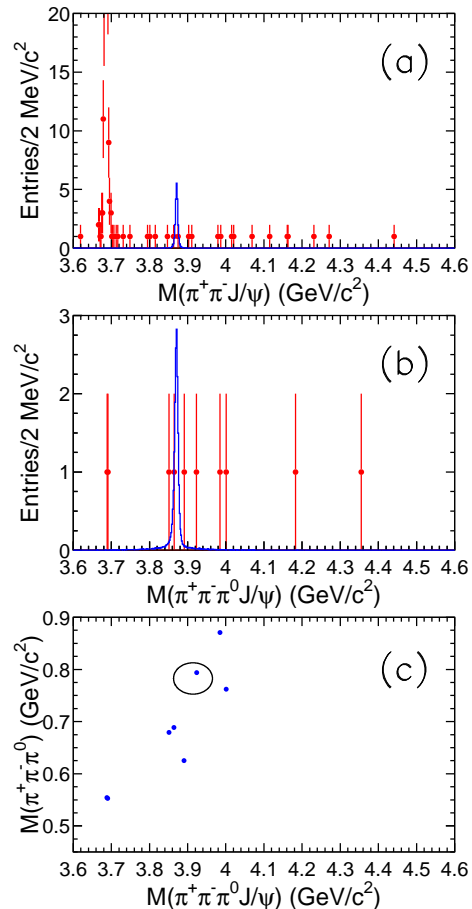


FIG. 4: (color online). (a) Distribution of the  $\pi^+\pi^- J/\psi$  invariant mass for  $\Upsilon(2S) \rightarrow \gamma_{\text{R}} \pi^+\pi^- J/\psi$  candidates. (b) Distribution of the  $\pi^+\pi^-\pi^0 J/\psi$  invariant mass for  $\Upsilon(2S) \rightarrow \gamma_{\text{R}} \pi^+\pi^-\pi^0 J/\psi$  candidates. (c) Scatter plots of  $m(\pi^+\pi^-\pi^0 J/\psi)$  versus  $m(\pi^+\pi^-\pi^0)$ , where the region indicated by the ellipse corresponds to the  $\pm 3\sigma$  mass regions of  $m(\pi^+\pi^-\pi^0 J/\psi)$  and  $m(\pi^+\pi^-\pi^0)$  from the  $X(3915) \rightarrow \omega J/\psi$  decay. Points with error bars are data, open histograms are the MC expectation for the  $X(3872)$  signal (arbitrary normalization). The peak at  $3.686$   $\text{GeV}/c^2$  in (a) is due to  $\psi(2S)$  production via ISR.

Several sources of systematic uncertainties are considered. The uncertainty due to particle identification efficiency is 2.4%-3.4% and depends on the final state particles. The uncertainty in the tracking efficiency for tracks with angles and momenta characteristic of signal events is about 0.35% per track, and is additive. The photon reconstruction contributes an additional 2.0% per photon. Errors on the branching fractions of the intermediate states are taken from the PDG [19]; they are 6.9% for the  $\chi_{c0}$  mode, 4.5% for the  $\chi_{c1}$  mode, 4.2% for the  $\chi_{c2}$  mode, 1.7% for the  $\gamma\psi(2S)$  mode, 24% for the  $\eta_c$  mode, 1.0% for the  $X(3872)$  mode, 1.3% for the  $X(3915)$  mode, and 1.6% for the  $\phi J/\psi$  mode. By using a phase space distribution and including possible intermediate resonant states, the largest difference of efficiency is determined to be 2.1% for the  $\eta_c$  decay modes. The

difference in the overall efficiency for a flat angular distribution of radiative photons and a  $1 \pm \cos^2 \theta$  distribution is less than 3.0%. Therefore, we quote an additional error of 5.0% due to the limited knowledge of the decay dynamics for all the states studied, except for the  $\chi_{c0}$  mode and  $\eta_c$  mode, which are known to follow a  $1 + \cos^2 \theta$  distribution. According to MC simulation, the trigger efficiency is 89% for the  $\chi_{cJ}$  mode, rather high for other modes ( $\geq 99\%$ ); we take a 3.0% error for the  $\chi_{cJ}$  mode and 1.0% error for other modes as a conservative estimate of the corresponding uncertainties. With the pure  $e^+e^- \rightarrow \gamma_{\text{ISR}}\psi(2S), \psi(2S) \rightarrow \pi^+\pi^- J/\psi$  or  $J/\psi\eta(\rightarrow \gamma\gamma)$  samples obtained from Belle data, the uncertainty due to the recoil mass squared requirement is 1.0% for the channels with a single photon and 4.7% for channels with two photons. By changing the order of the background polynomial, the range of the fit, and the values of the masses and widths of the resonances, uncertainties on the  $\chi_{cJ}$  and  $\eta_c$  signal yields are estimated to be 1.1% and 16%, respectively. In the  $\Upsilon(2S) \rightarrow \gamma_{\text{R}}\chi_{cJ}$  mode, the uncertainty associated with the requirement on the number of photons is 2.0% after applying a correction factor of 0.94 to the MC efficiency, which is determined from a study of a very pure  $\Upsilon(2S) \rightarrow \mu^+\mu^-$  event sample. In the  $\eta_c \rightarrow K_S^0 K^+ \pi^- + c.c.$  mode, the uncertainty in the  $K_S^0$  selection efficiency is determined by a study on a large sample of high momentum  $K_S^0 \rightarrow \pi^+\pi^-$  decays; the efficiency difference between data and MC simulation is less than 4.9% [21]. Finally, the uncertainty on the total

number of  $\Upsilon(2S)$  events is 2.3%. Assuming that all of these systematic error sources are independent, we add them in quadrature to obtain a total systematic error as shown in Table I.

Since there is no evidence for signals in the modes studied, we determine upper limits on the branching fractions of  $\Upsilon(2S)$  radiative decays. Table I lists the upper limits  $n^{\text{up}}$  for the number of signal events, detection efficiencies, systematic errors, and final results for the upper limits on the branching fractions. In order to calculate conservative upper limits on these branching fractions, the efficiencies are lowered by a factor of  $1 - \sigma_{\text{sys}}$  in the calculation.

To summarize, we find no significant signals for the  $\chi_{cJ}$  or  $\eta_c$ , as well as for the  $X(3872), X(3915), Y(4140)$ , or  $X(4350)$  in  $\Upsilon(2S)$  radiative decays. The results obtained on the  $\chi_{cJ}$  and  $\eta_c$  production rates are consistent with the theoretical predictions of [4].

We thank the KEKB group for excellent operation of the accelerator, the KEK cryogenics group for efficient solenoid operations, and the KEK computer group and the NII for valuable computing and SINET4 network support. We acknowledge support from MEXT, JSPS and Nagoya's TLPRC (Japan); ARC and DIISR (Australia); NSFC (China); MSMT (Czechia); DST (India); MEST, NRF, NSDC of KISTI, and WCU (Korea); MNiSW (Poland); MES and RFAAE (Russia); ARRS (Slovenia); SNSF (Switzerland); NSC and MOE (Taiwan); and DOE (USA).

- 
- [1] For a recent review, see N. Brambilla *et al.*, Eur. Phys. J. C **71**, 1534 (2011).
- [2] J. L. Rosner *et al.* (CLEO Collaboration), Phys. Rev. Lett. **95**, 102003 (2005).
- [3] M. Ablikim *et al.* (BESIII Collaboration), Phys. Rev. Lett. **104**, 132002 (2010).
- [4] Y. J. Gao, Y. J. Zhang, and K. T. Chao, hep-ph/0701009 on  $\Upsilon(1S)$  decays, and private communication with K. T. Chao on  $\Upsilon(2S)$  decays.
- [5] S. K. Choi *et al.* (Belle Collaboration), Phys. Rev. Lett. **91**, 262001 (2003).
- [6] S. Uehara *et al.* (Belle Collaboration), Phys. Rev. Lett. **104**, 092001 (2010).
- [7] T. Aaltonen *et al.* (CDF Collaboration), Phys. Rev. Lett. **102**, 242002 (2009).
- [8] C. P. Shen *et al.* (Belle Collaboration), Phys. Rev. D **82**, 051504(R) (2010).
- [9] C. P. Shen *et al.* (Belle Collaboration), Phys. Rev. Lett. **104**, 112004 (2010).
- [10] T. Barnes, S. Godfrey, and E. S. Swanson, Phys. Rev. D **72**, 054026 (2005); Y. Jia, W. L. Sang, and J. Xu, arXiv:1007.4541[hep-ph].
- [11] A. Abashian *et al.* (Belle Collaboration), Nucl. Instr. Meth. A **479**, 117 (2002).
- [12] S. Kurokawa and E. Kikutani, Nucl. Instr. Meth. A **499**, 1 (2003), and other papers included in this volume.
- [13] D. Besson *et al.* (CLEO Collaboration), Phys. Rev. D **76**, 072008 (2010).
- [14] T. Sjostrand *et al.*, Comput. Phys. Commun. **178**, 852 (2008).
- [15] E. Nakano, Nucl. Instr. Meth. A **494**, 402 (2002).
- [16] K. Hanagaki *et al.*, Nucl. Instr. Meth. A **485**, 490 (2002).
- [17] A. Abashian *et al.*, Nucl. Instr. Meth. A **491**, 69 (2002).
- [18] F. Fang, Ph.D thesis, University of Hawaii, 2003.
- [19] K. Nakamura *et al.* (Particle Data Group), J. Phys. G **37**, 075021 (2010).
- [20] C. Z. Yuan *et al.* (Belle Collaboration), Phys. Rev. Lett. **99**, 182004 (2007).
- [21] S.-W. Lin *et al.* (Belle Collaboration), Phys. Rev. Lett. **99**, 121601 (2007).

TABLE I: Summary of the limits on  $\Upsilon(2S)$  radiative decays to charmonium and charmonium-like states  $R$ . Here  $n^{\text{up}}$  is the upper limit on the number of signal events,  $\varepsilon$  is the efficiency with the secondary decay branching fractions excluded and trigger efficiency included,  $\sigma_{\text{sys}}$  is the total systematic error, and  $\mathcal{B}(\Upsilon(2S) \rightarrow \gamma R)^{\text{up}}$  ( $\mathcal{B}_R$ ) is the upper limit at the 90% C.L. on the decay branching fraction in the charmonium state case, and on the product branching fraction in the case of a charmonium-like state.

State ( $R$ )	$n^{\text{up}}$	$\varepsilon(\%)$	$\sigma_{\text{sys}}(\%)$	$\mathcal{B}_R$
$\chi_{c0}$	2.8	14.2	10.9	$1.0 \times 10^{-4}$
$\chi_{c1}$	3.1	14.8	10.8	$3.6 \times 10^{-6}$
$\chi_{c2}$	7.6	15.2	10.7	$1.5 \times 10^{-5}$
$\eta_c$	44	22.7	30	$2.7 \times 10^{-5}$
$X(3872) \rightarrow \pi^+ \pi^- J/\psi$	3.6	27.3	7.4	$0.8 \times 10^{-6}$
$X(3872) \rightarrow \pi^+ \pi^- \pi^0 J/\psi$	4.2	10.3	9.6	$2.4 \times 10^{-6}$
$X(3915) \rightarrow \omega J/\psi$	4.4	10.5	9.6	$2.8 \times 10^{-6}$
$Y(4140) \rightarrow \phi J/\psi$	2.3	22.3	7.4	$1.2 \times 10^{-6}$
$X(4350) \rightarrow \phi J/\psi$	2.3	21.0	7.4	$1.3 \times 10^{-6}$